Electrical Power and Energy Systems 143 (2022) 108481

Contents lists available at ScienceDirect

International Journal of Electrical Power and Energy Systems

journal homepage: www.elsevier.com/locate/ijepes

Dynamically robust coordinated set point tracking of distributed DERs at point of common coupling

Mazheruddin Syed [a,*], Ali Mehrizi-Sani [b], Maria Robowska [a], Efren Guillo-Sansano [c], Dong Wang [d], Graeme Burt [a]

[a] Institute for Energy and Environment, University of Strathclyde, Glasgow, Scotland
[b] Bradley Department of Electrical and Computer Engineering, Virginia Tech, Blacksburg, VA, USA
[c] Enercoop, Alicante, Spain
[d] Zeijhang University of Science and Technology, Zheijang, China

ARTICLE INFO

Keywords:
Ancillary services
Coordinated control
Distributed energy resources
Microgrids
Predictive control

ABSTRACT

Low-inertia operation of small-scale power systems, such as a microgrid or a portion of a long feeder, requires careful coordination of the controller performance of the constituting devices. This challenge is exacerbated in microgrids serving the functionalities of a conventional synchronous-based generation unit while comprised of smaller DERs operating mainly interfaced through power electronics converters. This paper builds on the idea of set point modulation and proposes a two-level control strategy that aims to achieve superior performance at the point of common coupling (PCC) of microgrids by combining a local control level with a distributed and coordinated level. Several case studies on both AC and DC systems, the CIGRE low-voltage benchmark system as the AC system and a test DC microgrid, validate the performance of the proposed approach. The real-world applicability of the approach is established via a high-fidelity power hardware-in-the-loop (PHIL) experimental setup and an application case study on grid frequency regulation. The proposed approach enables a microgrid to participate in ancillary service provisions where speed and quality of regulation are critical.

1. Introduction

With the rapid decommissioning of larger conventional fossil fuel based generation units around the world (specially coal), the transmission system operators (TSO) face an imminent challenge to operate the grid with minimal inertia [1]. The system frequency is expected to deviate faster during imbalance events (such as loss of generation), and there is an elevated risk of failure to maintain the frequency within statutory limits, leading to significant increase in operational costs [2]. This has necessitated the development of fast frequency response services to ensure the restriction of frequency within acceptable limits while allowing time for slower devices to be deployed [3]. The expected large-scale penetration of controllable distributed energy resources (DER) within the distribution networks in the near future presents the TSO with an opportunity to rely on a number of these assets for the procurement and delivery of appropriate ancillary services [4]. Many examples of utilization of DERs for ancillary service provision can be found in literature: frequency control in [5], voltage support in [6], power quality improvement in [7], power loss optimization in [8], and coordination of capacity at the interface of distribution and transmission in [9]. However, the coordination and control of such devices remain a challenge.

The fastest deployment of reserves is through decentralized control, i.e., participating devices respond to deviations in frequency based on local measurements [10,11]. Such approaches are also referred to as uncoordinated approaches due to the fact that the settings of participating devices are not updated online. However, smart devices responding simultaneously to frequency deviations can cause frequency oscillations and loss of load diversity [12]. Real-time or online control for reserve activation is enabled through centralized and distributed control approaches. The use of aggregated thermostatic, deferrable, and flexible loads, such as commercial buildings and fleets of electric vehicles, to follow a given power set point from TSO (centralized control), usually at a point of common coupling (PCC) such as the substation, is demonstrated in literature [13–15]. These control strategies, however, assume a geographically restricted cluster of DERs, often connected at one electrical node. An alternative approach for the control of geographically dispersed DERs in a microgrid is through market

* Corresponding author.
E-mail addresses: mazheruddin.syed@strath.ac.uk (M. Syed), mehrizi@vt.edu (A. Mehrizi-Sani), efren.guillo@enercoop.es (E. Guillo-Sansano), d.wang@zust.edu.cn (D. Wang).

https://doi.org/10.1016/j.ijepes.2022.108481
Received 26 January 2022; Received in revised form 9 June 2022; Accepted 10 July 2022
Available online 3 August 2022

facilitators such as load aggregators or virtual power plants (VPP) [16–19]. Distributed control approaches employing sparse communication are preferred to ensure resiliency by avoiding single point of failure and to ensure robustness under communications failures. Analysis of communications requirements of a VPP can be found in [20]; a robust design considering cyber attacks has been discussed in [21]. Real-time control of DERs through a VPP is discussed in the literature; some do not take participating DER output measurement as feedback [22], while a few do consider the feedback for accurate set point tracking [23,24].

Due to the varied response characteristics of participating individual DERs, the cumulative response at the PCC may exhibit poor dynamic behaviour. This can be in the form of slow aggregated cumulative response, oscillations representative of lightly damped response, or unexpected overshoots. Coordinating the response characteristics of individual DERs to improve the cumulative dynamic response during frequency events is desirable, particularly for systems with low inertia. Some studies have explored the composition of a VPP, i.e., the optimal sizing and siting of DERs through analytical [25], numerical [26], and heuristic [27] methods. The power allocation problem for varied applications (including VPPs) has been discussed, where the response speeds of DERs are taken into design consideration [28,29]. This enables effective utilization of participating DER characteristics to support set point regulation. However, the limitations of such approaches include: (i) the requirement of operational knowledge of the participating DERs, (ii) being an offline approach that does not take DER response as feedback and therefore is only able to improve the speed of response but not eliminate any other undesired dynamic behaviours, and (iii) can be computationally expensive, which in turn limits the real-time application of the approach.

Recognizing these gaps, this paper proposes an approach to ensure dynamically robust set point regulation as a VPP. This paper builds upon the set point modulation (SPM) approach proposed in [30–32]. The contributions of this paper are as follows:

- A two-level coordinated SPM approach is proposed where the individual response characteristics of participating DERs are harnessed to provide enhanced dynamic response at the PCC. The approach does not rely on prior knowledge of the participating DERs and is capable of robust set point regulation in real time, mitigating any undesired behaviour in dynamic response. Furthermore, this approach is agnostic to the secondary-level control strategy and specifically how the reference set points are generated. Such effective control enables greater potential for participation of DERs in ancillary service provision, presenting a major benefit for DER owners and aggregators.
- The proposed approach has been evaluated within representative AC and DC networks independently, where the deployment of the proposed control is anticipated in the future to support frequency regulation in low-inertia power systems.
- The real-world applicability of the proposed approach is demonstrated by means of its validation using high-fidelity power hardware-in-the-loop experimental setup at the Dynamic Power Systems Laboratory at the University of Strathclyde. This verifies the real-time operation of the proposed approach and its ability to deal with nonidealities that can be encountered when deployed in practice.

The remainder of the paper is organized as follows: the proposed coordinated set point modulation approach is presented in Section 2. The performance of the proposed approach is thoroughly evaluated by its incorporation within a low-voltage AC distribution network and a DC microgrid in Section 3. To appraise its technology readiness level to bolster its feasibility for real-world adoption and roll-out, a power hardware-in-the-loop (PHIL) experimental validation is undertaken in Section 4. An application oriented case study demonstrating the potential role of the proposed approach in grid frequency regulation is presented in Section 5. Section 6 presents a directions for future research by means of a discussion. Section 7 concludes the paper.

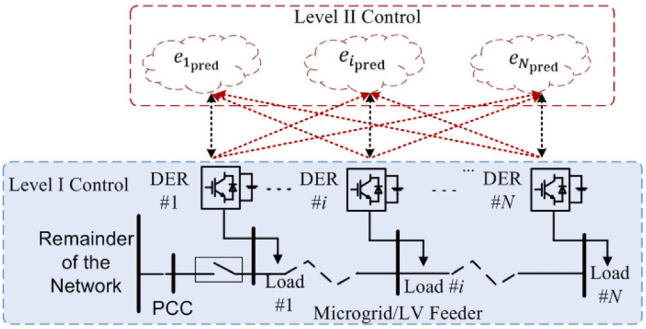

Fig. 1. Sample microgrid/low voltage feeder network.

2. Coordinated set point modulation

2.1. Background

SPM refers to an approach that monitors the deviation of the system response $x(t)$ from its reference set point x_{sp} and modulates the original set point as

$$x'_{\text{sp}} = x_{\text{sp}} + me(t) \tag{1}$$

where x'_{sp} is the modified set point, m is a design parameter reflecting the impact of the set point modulation, and $e(t)$ is the tracking error calculated as

$$e(t) = x_{\text{sp}} - x(t). \tag{2}$$

The term set point here refers to the controlled variable. For a PI-based controller, from a control theory point of view, this has an effect similar to increasing the proportional gain to increase the controller speed without the consequent deteriorating increase in overshoot. To further improve the dynamic response of the system, i.e., to have a shorter settling time and smaller overshoots, the tracking error is replaced by a prediction of the dynamic trajectory of the error $\hat{e}_{\text{pred}}$ as:

$$x'_{\text{sp}} = x_{\text{sp}} + m\hat{e}_{\text{pred}}(t) \tag{3}$$

The concept of SPM for dynamic response improvement was first proposed in [33]. Conventionally designed for improving the dynamic response of an individual device, it has been proven effective in dynamic response improvement of DER as reported in [34] and that of an electric drive in [35]. With the foreseen penetration of DERs in a network, the incorporation of such an approach without coordination leads to an inefficient operation of the system. Furthermore, the individual DER improved response might not be in the global interest of the network within which the DERs operate. This is the premise of the proposed coordinated SPM approach as will be further detailed in the following subsections.

2.2. Proposed approach

This section presents the proposed approach, implemented as a two level control, in detail. Consider the sample network, representing either a low voltage (LV) feeder or a microgrid, with N controllable DERs (denoted by $i = 1, 2, \ldots, N$) as shown in Fig. 1. Representing the sample network as a complex-weighted graph $\chi = (v_\chi, \varepsilon_\chi)$, the vertices $v_\chi = \{v_1, v_2, \ldots, v_N\}$ are the DER interconnected buses and edges $\varepsilon_\chi \subseteq v_\chi \times v_\chi$ represent their electrical interconnections. We assume that M DERs, $M \subset N$, are contracted by a VPP to provide ancillary services to the TSO through the PCC.

Given a disturbance within the network, P_M is the total reserve activation requested by the VPP from the M contracted DERs.

2.2.1. Communications network

The communications network is represented by an undirected graph $\varrho = (v_\varrho, \varepsilon_\varrho)$, where vertices $v_\varrho = \{v_1, v_2, \ldots, v_M\}$ correspond to the M vertices in χ. The edges $\varepsilon_\varrho \subseteq v_\varrho \times v_\varrho$ represent communications links for the exchange of data and are not necessarily the same as electrical connections in χ. The adjacency matrix for the communications network under consideration can be represented as $A = [a_{ij}] \subseteq \mathbb{R}^{n\times n}$, where a_{ij} represents the connectivity of two DERs i and j. The element $a_{ij} = 1$ if DERs i and j exchange information via connected edge $(v_i, v_j) \in \varepsilon_\varrho$, else $a_{ij} = 0$. The M DERs receive a set point from the VPP (can be observed as virtual leader with index 0) and therefore, the pinning matrix can be defined as $G = \text{diag}[g_i] \subseteq \mathbb{R}^{n\times n}$, where gain $g_i = 1$ for a working communications link.

2.2.2. Level I independent control

Level I control, also referred to as independent control, improves the dynamic response of the individual DERs. With P_M as the requested reserves from the participating DERs, the accumulated response can be represented as

$$P_M = \sum_{i=1}^{M} g_i p_{i_{\text{sp}}}(t) \tag{4}$$

where $p_{i_{sp}}$ represents the set point of the ith participating DER. Incorporating SPM for independent operation, the set point of the ith DER is modified as

$$p'_{i_{\text{sp}}}(t) = p_{i_{\text{sp}}} + u_i^I(t) \tag{5}$$

where u_i^I is the modulation factor of level I control defined as

$$u_i^I(t) = m_i \times \hat{e}_{i_{\text{pred}}}(t). \tag{6}$$

This paper employs a linear predictor for prediction of error trajectory due to its suitability for real-time implementation with minimum computational effort and simple implementation. The error in power over prediction horizon T_{pred} is

$$\hat{e}_{i_{\text{pred}}}(t_0 + T_{\text{pred}}) = e_i(t_0) + r(t_0)T_{\text{pred}} \tag{7}$$

where $r(t_0)$ is the average rate of change calculated over past measurements based on least squares error. To limit the buffer requirement for real-time implementation, the measurement history is limited to one data point (history term) equal to the prediction horizon, resulting in the current value of $e_i(t)$ being equal to the average of the history term and the predicted term:

$$\hat{e}_{i_{\text{pred}}}(t_0 + T_{\text{pred}}) = 2e_i(t_0) - e_i(t_0 - T_{\text{pred}}) \tag{8}$$

In a change from conventional implementation of SPM, the error tolerance band is eliminated given DERs under consideration are interfaced via power electronics. The tolerance band is traditionally implemented when devices under consideration are susceptible to a frequent change in set point.

2.2.3. Level II coordinated control

For the purpose of coordinated operation, the level I control is complemented with a distributed implementation, i.e., information from participating DERs is shared amongst each other. The objective is to ensure fast and improved dynamic response at the PCC, where the sum of the responses from participating DERs is observed, rather than dynamically improved local response of the individual participating DER. The set point of the ith DER is therefore modified as

$$p''_{i_{\text{sp}}}(t) = p_{i_{\text{sp}}} + u_i^I(t) + u_i^{II}(t) \tag{9}$$

where u_i^{II} is the modulation factor of level II control:

$$u_i^{II}(t) = m_i \sum_{j=1, j\neq i}^{M} a_{ij}\hat{e}_{j_{\text{pred}}}(t) \tag{10}$$

Table 1
Average time delays within Great Britain [39].

	Bristol	Manchester	Newcastle	Edinburgh
Distance to London	189.3 km	335.3 km	447.3 km	638 km
Delay to London	4.341 ms	6.283 ms	6.073 ms	11.451 ms

where $\hat{e}_{j_{\text{pred}}}(t)$ is the predicted error of jth DER. Substituting and rearranging, (9) can be represented as

$$p''_{i_{\text{sp}}}(t) = p'_{i_{\text{sp}}}(t) + u_i^{II}(t) \tag{11}$$

2.3. Design and implementation considerations

2.3.1. Architectural flexibility

The proposed approach offers architectural flexibility in its implementation. For the objective at hand, i.e., to ensure improved dynamic response at the PCC, the following three implementations are feasible: (i) a centralized implementation with the proposed control incorporated within the VPP, (ii) a hierarchical implementation where there is a central LV network controller or microgrid controller between the VPP and participating DER (such as distributed energy resource management systems [DERMS]), or (iii) a fully distributed implementation with DERs communicating with each other.

2.3.2. Communications

Analogous to many other distributed control approaches, the proposed approach relies upon the existence of a suitable communication network. Guidance on development of communications network for distributed control can be found in [36], while guidance specifically on wireless networks can be found in [37]. The performance of such a control system is characterized by three main properties (i) timeliness, (ii) availability, and (iii) accuracy of data [38]. Timeliness refers to the time delays associated with communications among neighbouring participants, the data availability refers to the efficient use of limited communication bandwidth, and data accuracy refers to any cybersecurity issues. The target application of the approach and its corresponding design features cater for the three properties to a desired level to ensure appropriate control as described below.

The proposed approach employs event-triggered communication where the exchange of information is initiated when a corresponding power regulation command is received from the aggregator. This significantly reduces the requirement of continuous real-time communication. Additionally, with only one parameter exchange, the burden on communications infrastructure remains low. The average inter-city time delay within Great Britain is presented in Table 1. With time delays between major cities in the order of milli-seconds, the delay within a microgrid or an LV feeder is expected to be in the order of micro-seconds. Finally, the proposed approach is robust to single points of communication failure and resilient to complete communications failure, where the implementation would resort to the level I implementation where

$$p''_{i_{\text{sp}}}(t) = p'_{i_{\text{sp}}}(t). \tag{12}$$

2.3.3. Parameter selection

By implementation and design, the SPM approach is adaptive to ensure that the parameter selection does not present a challenging task. Two parameters for the control need selection, and the following discussion presents practice adopted through theoretical analysis and practical experience.

Scaling factor m. A detailed discussion on the impact of m on the performance of an individual apparatus is presented in [34,40] complemented by an analytical discussion in [33]. However, for the coordinated approach, no further tuning is required. As long as the decentralized implementation is satisfactory, the coordinated approach will lead to satisfactory performance.

Prediction horizon T_{pred}. The choice of prediction method minimally impacts the performance of the proposed approach, however a simpler predictor is preferable for real-time applications due to computational constraints. As for the prediction horizon, a heuristic rule of thumb that yields best results is $T_{\text{pred}} = 10 \times 2\pi/\omega_0$, where ω_0 is dominant system natural frequency.

2.3.4. Stability

The incorporation of SPM approach within a control apparatus (such as the DER) was shown not to impact the stability of the DER itself [33]. However, the SPM approach utilized was that of a block modulation, where the sum of two consequent changes in set point is equal to zero. The proposed approach employs modulation of set point based on the linear extrapolation of error signal. Due to the discrete implementation in real time, changes in set points for a step change in reference set point can be represented as the summation of time shifted unit step functions as

$$p'(t) = u(t - t_0) + \sum_{i=1}^{n} ku(t - t_i) \tag{13}$$

where $k = me_{\text{pred}}$, t_0 is the time at which the step change in reference is initiated, t_i is the representation of monotonically increasing sequence, and n represents the number of set point changes. Eq. (13) in Laplace domain is

$$P'(s) = \frac{1}{s} + k \sum_{i=1}^{n} \frac{e^{-st_i}}{s} \tag{14}$$

Denoting the transfer function of the DER as $H(s)$ and the measured output real power as $p_m(t)$, the Laplace transform can be represented as

$$P_m(s) = H(s)P'(s) \tag{15}$$

Following the final value theorem

$$\begin{aligned} \lim_{t\to\infty} p_m(t) &= \lim_{s\to 0} sP_m(s) \\ &= \lim_{s\to 0} sH(s)P'(s) \\ = \lim_{s\to 0} sH(s) &\left(\frac{1}{s} + k \sum_{i=1}^{n} \frac{e^{-st_i}}{s} \right) \\ = \lim_{s\to 0} H(s) &\lim_{s\to 0} \left(1 + k \sum_{i=1}^{n} e^{-st_i} \right) \end{aligned} \tag{16}$$

Therefore, for $\lim_{t\to\infty} p_m(t) = 1$, two necessary conditions arise:

$$\begin{cases} \lim_{s\to 0} sH(s) = 1 \\ k \sum_{i=1}^{n} e^{-st_i} = 0 \end{cases} \tag{17}$$

The proposed SPM approach ensures the final set point to the DER is equivalent to its reference set point. Therefore, the incorporation of the proposed SPM approach within a DER does not impact the stability of the DER as long as the DER is stable before the augmentation of the SPM itself.

3. Performance evaluation

The superior performance and applicability of the proposed coordinated SPM control is demonstrated within a LVAC distribution network and a DC microgrid. A DER in a microgrid can operate in grid-forming mode [41] or in grid-following mode (PQ control mode [42]). Grid-forming control modes are adopted to support islanded operation of the microgrid, while the majority of the DERs connected to the power grid operate in PQ control mode, controlling their real and reactive power outputs. The performance of the proposed coordinated SPM is therefore assessed for the following three scenarios within the context of battery energy storage system (BESS) DER operating in PQ mode, and participating within a VPP for ancillary service provision.

- **Simultaneous set point Change:** This event represents a request of activation of reserves from a VPP distributed among the participating DER. The assumption is the request of activation is made at the same time, and therefore referred to as a simultaneous change in set point.
- **Staggered set point Change:** This event is complementary to the simultaneous change in set point where the activations are separated in time, i.e., the activation requests are sent at different points in time.
- **External Disturbance:** This represents a scenario where the performance of the control is assessed when the participating DER are providing the requested reserves and the network is subject to a transient.

To assist the performance evaluation of the proposed coordinated SPM, three key indicators have been defined as:

- **Settling time:** The time elapsed from when the signal of interest $x(t)$ digresses from within the defined error band ϵ, subject to an external disturbance or a step change in the reference set point, to when $x(t)$ returns and remains within ϵ is referred to as the settling time T_{set} and represented as:

$$\begin{aligned} T_{\text{set}} = \text{argmin}\{T_{\text{set}} \in \mathcal{R} \mid \forall\, t > T_{\text{set}} : \\ x_{\text{band}}^{\text{upper}} < x(t) < x_{\text{band}}^{\text{lower}}\} \end{aligned} \tag{18}$$

- **Overshoot:** Defining the maximum excursion of $x(t)$ subject to an external disturbance or after a step change in the reference set point as x_{max}, the overshoot is

$$x_{\text{os}} = \left| \frac{x_{\text{max}} - x_{sp}}{x_{sp}} \right| \tag{19}$$

- **Cumulative tracking error:** The sum of the tracking errors at every time step T_s from the initiation of the external disturbance or step change in reference to the time when the measured output signal has settled (i.e., T_{set}) is referred to as cumulative tracking error (CTE) calculated as:

$$S_e = \sum_{k=0}^{N} \left| x_{\text{sp}}[k] - x[k] \right| \tag{20}$$

where $N = T_{\text{set}}/T_s$. A smaller S_e corresponds to better performance.

In the rest of this section, the performance of the proposed control is assessed in comparison to a reference controller without SPM. To further demonstrate the added value through the coordination, the performance is also benchmarked against the independent (level I only) implementation of SPM.

3.1. Low-voltage AC distribution network

The CIGRE Benchmark Systems for Network Integration of Renewable and Distributed Energy Resources is chosen as the test AC network, a simplified diagram of which is shown in Fig. 2 [43]. The network incorporates the important technical characteristics of public distribution networks with respect to its structure, symmetry, substation connection, protection, line types and earthing as detailed in [44]. The network comprises of three feeders, residential, commercial, and industrial, tapped from an on load tap changer with 5% regulation capacity at the primary side of 20 kV. The residential feeder is 0.4 kV overhead line serving a suburban residential area with six buses accommodating both single phase and three phase customers. The DERs at buses 1–4 are rated at 10 kW each representing a complementary storage installed to maximize energy utilization from photovoltaics. The DER at bus 5 represents an electric vehicle charging station, rated at maximum power of 30 kW (fast charging).

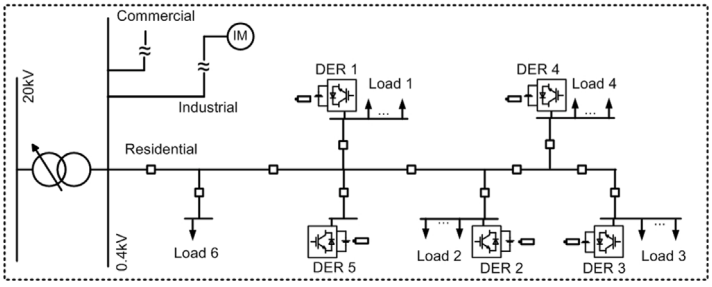

Fig. 2. LVAC distribution network.

Table 2
Key indicators for performance evaluation of proposed control within a LV distribution network.

	Simultaneous set point change[a]						Staggered set point change[b]						External disturbance					
	No SPM		Independent		Coordinated		No SPM		Independent		Coordinated		No SPM		Independent		Coordinated	
	x_{os}	T_{set}	x_{os}	T_{set}	x_{os}	T_{set}	x_{os}	T_{set}	x_{os}	T_{set}	x_{os}	T_{set}	x_{dev}	T_{set}	x_{dev}	T_{set}	x_{dev}	T_{set}
DER 1	23.12	0.76	13.36	0.55	11.85	0.54	22.53	0.82	13.24	0.63	16.52	0.72	5.04	1.95	2.27	1.93	2.02	1.95
DER 2	61.12	0.54	49.20	0.46	35.83	0.45	56.56	0.78	46.53	0.67	23.13	0.75	6.35	0.92	3.10	0.68	2.67	1.32
DER 3	21.25	0.49	11.61	0.47	10.56	0.48	27.84	0.75	15.06	0.74	16.17	0.74	8.79	1.80	4.19	1.34	3.36	1.30
DER 4	19.56	0.51	17.52	0.43	18.34	0.43	25.43	0.75	16.31	0.74	11.33	0.74	6.56	1.60	3.19	1.29	1.54	1.04
DER 5	47.98	0.47	40.61	0.45	25.62	0.45	42.41	0.78	37.49	0.75	19.37	0.75	7.34	0.92	3.53	0.49	1.71	1.60
PCC	14.95	0.55	17.25	0.50	5.99	0.42	11.01	0.76	10.46	0.73	4.84	0.72	64.0	0.816	57.5	0.10	51.4	0.02

x_{os} is in %, T_{set} is in s.
[a]Results presented for simultaneous step change from 0 pu to 0.1 pu.
[b]The best performing step response results at PCC presented.

3.1.1. Simultaneous set point change

The performance for two changes in active power set point are evaluated, step up from 0 pu to 0.1 pu at $t = 0.5$ s and step down from 0.1 pu to 0 pu at $t = 2.5$ s. The individual responses of the DERs are presented in Fig. 3(a) with the aggregated active power response at PCC presented in Fig. 4(a). The key indicators to assess the performance of the control have been presented in Table 2, with the error band selected for the calculation of the settling time being 3%. As is evident, with no SPM each of the individual DERs present a relatively high overshoot with DER 2 exhibiting highest overshoot of 61%. Due to varied responses of individual DER, the overshoot at the PCC is about 14.95%. When independent SPM is incorporated, the individual DER response is improved in terms of both the overshoot and settling time, however, the overshoot at the PCC increases by about 2.3%. With the incorporation of coordinated control, the response of individual DERs and the aggregated response at the PCC improves both in terms of overshoot and settling time. The CTE over time for a simultaneous step increase in reference active power set point is shown in Fig. 4(b) which further reinforces the improvement in dynamics introduced by the coordinated approach — a 100% improvement compared to independent approach and 300% compared to conventional approach with no SPM. Therefore, it can be said that a independent approach improves local response of the individual DERs while a coordinated approach ensures improved response at the PCC. From the perspective of a VPP, the individual response of a DER is of less value but an improved aggregated response with much tighter regulation in comparison to reference commands is critical.

3.1.2. Staggered set point change

The response of the system when staggered set point changes are issued to individual DER units has been analysed with the three control approaches. The individual responses of the DER units to a step change in reference active power from 0 pu to 0.1 pu at $t = 4.5$ s for DER 1, at $t = 6.5$ s for DER 2 and DER 3 and a step change at $t = 8.5$ s for DER 4 and DER 5, are presented in Fig. 3(b) and the cumulative response at PCC in Fig. 4(a) (4 s–10 s). The results presented in Table 2 clearly presents the advantage of the independent and coordinated approaches over the conventional approach, each presenting a minimum improvement in overshoot of 10% and a moderate reduction in settling time of the individual units. From Fig. 4(a) the distinctive improvement in tighter power regulation at the PCC is evident, however, it must be noted that DERs that do not receive a change in set point still contribute to power regulation. This reflects the coordination, where all the units work towards improved dynamic performance at the PCC. The CTE for the three control approaches shown in Fig. 4(c) reveals a reduction of the error close to 50% when the coordinated algorithm is implemented in comparison with the independent approach for the staggered operation.

3.1.3. External disturbance

Irrespective of the network condition, a strict power regulation is expected by the VPP due to the fact that in most cases the services of a VPP are requested for critical ancillary service provision. Therefore, when subject to an external disturbance, the participating DERs of the VPP are expected to continue the provision of the requested amount of power; however, due to severity of the transient, the control of the DER might struggle to ensure regulation at the set point. The connection of the induction motor at the industrial feeder is the external disturbance under consideration. As no step change in reference set point is issued, the maximum deviation from the set point x_{dev} is calculated as the key indicator instead of the overshoot. The deviation in all the units can be seen from Fig. 3(c), which is due to the change in voltage on the feeder. The quantified deviations presented in Table 2 reveal that the approach without SPM suffers from instantaneous deviations from the set point of up to 87%. These deviations can be controlled to 50% with the use of the independent control approach and a further 5–15% when the coordinated control is implemented. These can also be observed in a more general manner from Fig. 4(c), where the reduction in error is significant.

3.2. DC microgrid

An LVDC network representative of last mile distribution network interconnection as proposed in [45] and utilized in [46,47] has been adapted for this study as in Fig. 5. The DC microgrid is interfaced to an AC grid through a two-level voltage source converter (VSC).

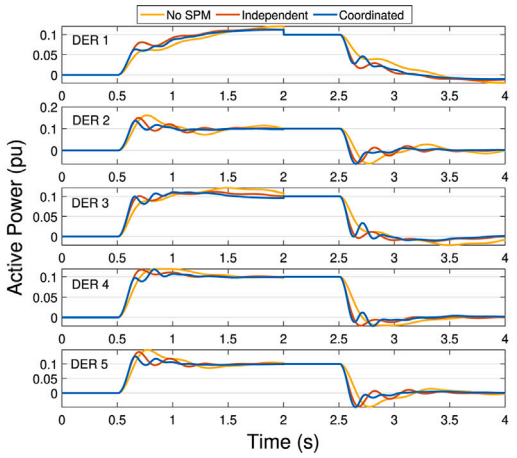

(a) Simultaneous set point change.

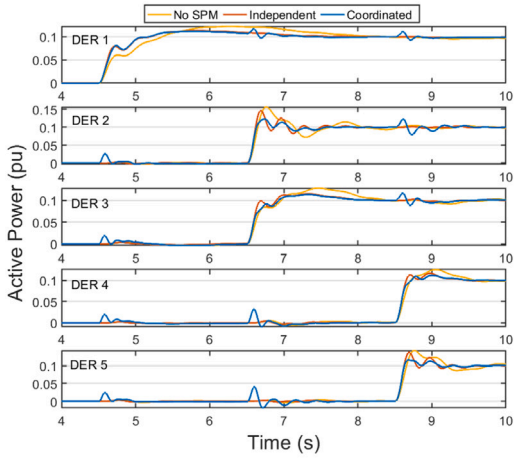

(b) Staggered set point change.

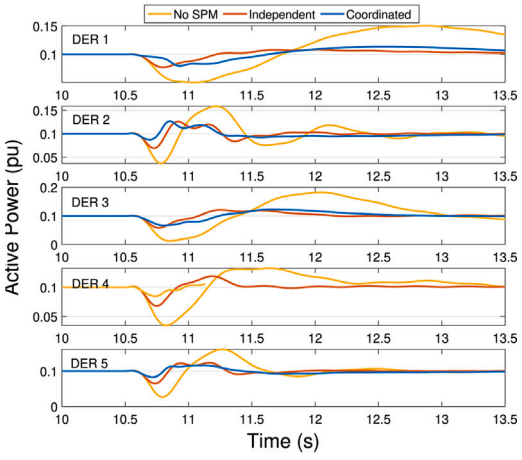

(c) External Disturbance.

Fig. 3. Performance evaluation within a low-voltage AC distribution network — individual DER response.

The VSC provides ±0.375 kV DC pole to pole voltage at PCC. The DC microgrid supplies end users through dual active bridge converters with four buses. The DERs at buses 1–4 are rated at 20 kW, 25 kW, 15 kW, and 20 kW, respectively, each representing energy storage technology (e.g., PV or Electric Vehicle)

For the DC microgrid, the same scenarios are considered, simultaneous step up and simultaneous step down are applied at $t = 0.3$ s

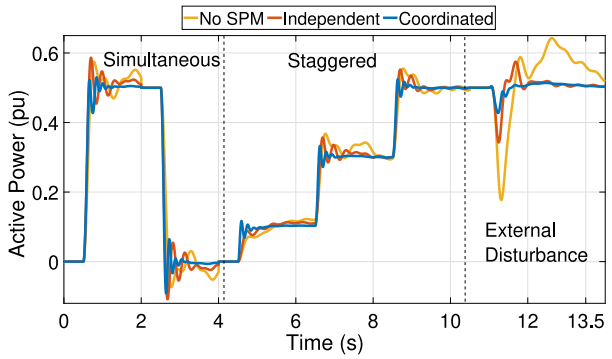

(a) Cumulative response at PCC.

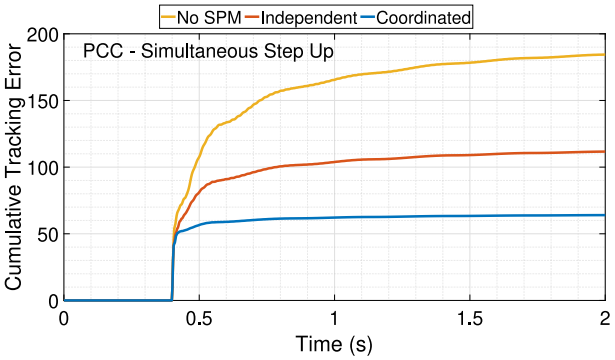

(b) CTE over time for simultaneous set point change - step up.

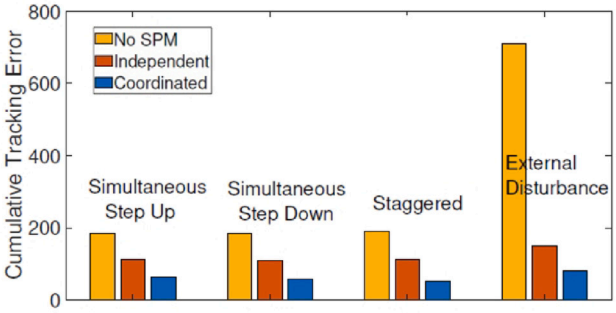

(c) CTE for scenarios under consideration.

Fig. 4. Performance evaluation within a LVAC distribution network — response at PCC.

and $t = 0.32$ s, staggered set point change is applied at $t = 0.35$ s, and external disturbance is applied at $t = 0.43$ s. The individual responses of the DERs along with the aggregated active power response at the PCC are presented in Fig. 6. The associated key indicators are presented in Table 3, with the error band selected for the calculation of the settling time as 3%.

In the simultaneous set point change scenario, with no SPM, each DER has relatively high overshoot, especially DER 3 with highest overshoot of 133.5%. With the implementation of independent SPM, the individual response of DERs is improved in terms of overshoot and settling time, resulting in reduction of overshoot at PCC from 38.89% to 0%. When the coordinated control is incorporated, similar reduction in overshoot at PCC is achieved in addition to smaller CTE as shown in Fig. 7, a 66.3% and 33.88% reduction compared to the cases without SPM and with independent SPM respectively.

For the staggered change in set point, each DER unit receives a step change request of 0 to their rated power — at $t = 0.35$ s for DER 1, $t = 0.37$ s for DER 2, $t = 0.39$ s for DER 3, and $t = 0.41$ s for DER 4 as shown in Fig. 6. Compared to the same scenario without SPM, implementation of independent SPM and coordinated SPM yields 3.4%–50.4%

Table 3
Key indicators for performance evaluation of proposed control within a DC microgrid.

	Simultaneous set point change[a]						Staggered set point change[b]						External disturbance					
	No SPM		Decentralized		Coordinated		No SPM		Decentralized		Coordinated		No SPM		Decentralized		Coordinated	
	x_{os}	T_{set}	x_{os}	T_{set}	x_{os}	T_{set}	x_{os}	T_{set}	x_{os}	T_{set}	x_{os}	T_{set}	x_{dev}	T_{set}	x_{dev}	T_{set}	x_{dev}	T_{set}
DER 1	69.35	12.3	19.5	2.8	0	3.5	10.25	8.3	6.8	5.6	6.2	5.6	150	20.9	80.55	17.2	63.65	17.5
DER 2	54.04	6.7	0	1.8	8.52	2.6	50.4	7.4	0	1.7	0	1.7	19.36	25.9	6.76	11.6	13.76	16.6
DER 3	133.5	10.3	30	6.9	50.5	6.9	45.5	18	10	11.2	10	9	84.06	35.4	39.1	25.7	31.8	27.7
DER 4	50	8.3	7.95	1.4	9.7	1.4	59.5	9.1	7.05	1.1	7.05	1.1	16.1	36.6	7.4	19.2	14.85	24.1
PCC	38.89	10.4	0	5	0	5	29.2	9.4	19.26	2.4	4.6	1.7	50.13	23.7	24.25	20.9	17.85	16.3

x_{os} is in %, T_{set} is in s.
[a]Results presented for simultaneous step change from 0 pu to 0.1 pu.
[b]The best performing step response results at PCC presented.

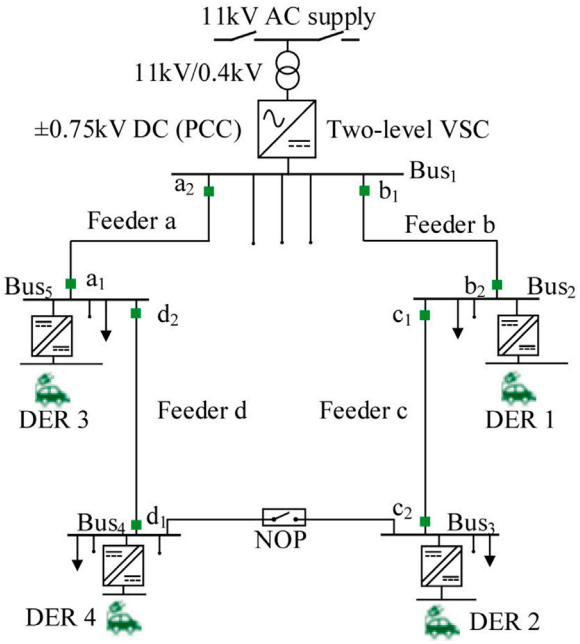

Fig. 5. An example of LVDC microgrid.

overshoot reduction, at the same time a 63% and 76.9% reductions in cumulative tracking error as shown in Fig. 7. The improvement of the dynamic response is also reflected in an external disturbance that is applied at $t = 0.43$ s. Table 3 shows that 9.7%–69.45% overshoot reduction is achieved when independent SPM is utilized. While PCC has a further 6.4% overshoot reduction with coordinated SPM.

4. Power hardware-in-the-loop experimental validation

To demonstrate the real world applicability of the proposed approach and to appraise its technology readiness level, a rigorous validation through high fidelity power hardware-in-the-loop (PHIL) experimental setup has been undertaken at the Dynamic Power Systems Laboratory at the University of Strathclyde. The LVAC distribution network utilized for performance evaluation within Section 4-A has been modified for PHIL experiment as shown in Fig. 8(a) in accordance with [48]. The power system is split in two, DER 3 represented by 15 kVA four quadrant converter emulating a BESS while the remainder of the network is simulated in real-time within the digital real-time simulator (DRTS) at a time step of 50 μs. The voltage from Bus 3 is reproduced within the laboratory using a 90 kVA four quadrant power amplifier, also responsible for measurement of the response current and feed it back to the DRTS. The proposed control is incorporated within the real-time target used for hosting the control algorithm of the 15 kVA four quadrant converter, operating with high fidelity measurements obtained at a sampling rate of 10 kHz. This presents a close to real-world implementation within a controlled environment, enabling validation that emboldens confidence in the proposed approach.

The performance of the hardware DER with conventional, independent and coordinated control approach subject to simultaneous step up, step down, staggered step change and external disturbance are presented in Fig. 8(b) (top). The cumulative power response at the PCC is shown in Fig. 8(b) (bottom). The accompanying key indicators for the PHIL evaluation are shown in Table 4. The results are in conformance with the results discussed in Sections 3.1 and 3.2, with level I only and coordinated approach demonstrating enhanced dynamic response in terms of overshoot and settling time. The CTE for cumulative power response at the PCC is shown in Fig. 8(c) where the advantage of the proposed approach is clearly brought forward.

The PHIL evaluation therefore demonstrates the capability of the proposed approach to (i) be synthesized within a micro-controller for operation in real-time and (ii) deal with non-ideal conditions such as measurement noise.

5. Application in grid frequency regulation

In this section, the advantage of the proposed approach in frequency regulation of a transmission network is demonstrated. A generic system frequency response model, tuned to reproduce Great Britain transmission network dynamics [49], is employed to emulate representative frequency response. The frequency from the emulator is used as an input for a frequency controlled voltage source connected to a LV microgrid (adapted based on the LVAC distribution network utilized in Section 3.1) as shown in Fig. 9. The description and chosen values of the parameters of the generic system frequency response emulator are presented in the Appendix, along with the adaptations to realize the LV microgrid from the LVAC distribution feeder.

A frequency event is emulated by introducing a power imbalance of 100 MW (ΔP_{event}). The aggregators activate and request response from the DERs when the system frequency reaches the lower threshold of the operating frequency, i.e., 49.8 Hz. The sum of power response from the DERs (ΣP_{MG}) within the microgrid is scaled by a scaling factor n and sent as an input to the generic system frequency response emulator. The active power response of the DERs and the consequent frequency profiles for the three cases, (i) no SPM, (ii) independent SPM and (iii) coordinated SPM is presented in Figs. 10(a) and 10(b) respectively. In addition, the sensitivity of the approach to changing system inertia is evaluated by incorporating three different values of inertia. For coordinated SPM approach, a communications delay of $Td = 0.5$ ms is incorporated.

As can be observed from Fig. 10(a), the improvement in active power response of the microgrid with incorporation of independent and coordinated SPM is evident under all inertial values considered. Consequently, the independent and coordinated SPM approaches improve the dynamic frequency response of the transmission system as shown in Fig. 10(b). Particularly of interest is the case when $H = 0.5H_0$ (representative of future with reduced inertia), the no SPM and independent

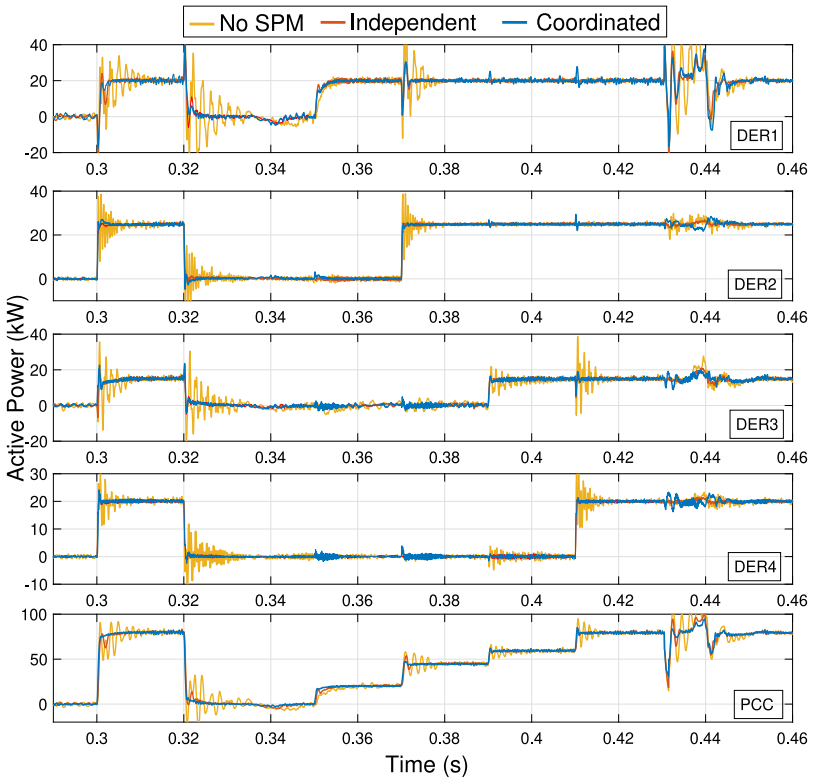

Fig. 6. Performance evaluation within a DC microgrid.

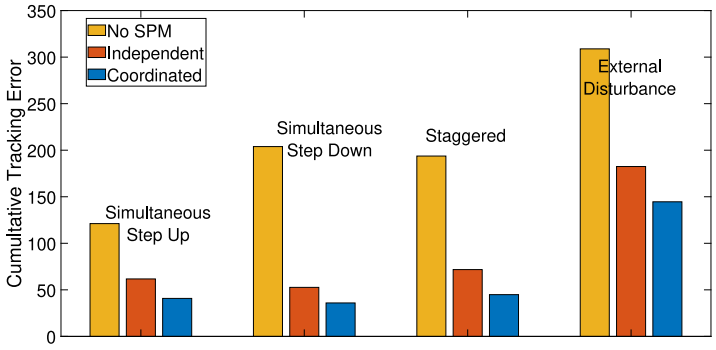

Fig. 7. CTE for scenarios under consideration — DC microgrid.

Table 4
Key indicators for performance evaluation of proposed control — PHIL implementation.

	Simultaneous set point change[a]						Staggered set point change[b]						External disturbance					
	No SPM		Independent		Coordinated		No SPM		Independent		Coordinated		No SPM		Independent		Coordinated	
	x_{os}	T_{set}	x_{os}	T_{set}	x_{os}	T_{set}	x_{os}	T_{set}	x_{os}	T_{set}	x_{os}	T_{set}	x_{dev}	T_{set}	x_{dev}	T_{set}	x_{dev}	T_{set}
DER 3	19.85	0.70	12.44	0.46	9.72	0.44	19.83	0.80	12.94	0.56	14.29	0.55	2.97	0.31	2.23	0.26	8.3	0.12
PCC	9.86	0.37	5.7	0.25	3.48	0.21	15.07	0.46	11.62	0.36	5.82	0.35	16.39	0.53	8.09	0.41	2.35	0.11

x_{os} is in %, T_{set} is in s.
[a]Results presented for simultaneous step change from 0 pu to 0.1 pu.
[b]The best performing step response results at PCC presented.

SPM approaches fail to regulate the frequency within the statutory limits defined as [49.5, 50.5] Hz. By coordinating the response of two fast acting DERs within each of the microgrid (constituting to 40% proportion), the coordinated SPM approach is capable of regulating the frequency within the statutory limits. This demonstrates the valuable role the proposed approach can play in the future ancillary service provision market within a renewable-rich power grid.

6. Discussion and future outlook

The proposed approach is the first contribution exploring the coordination of SPM to harness the mutual capabilities of DER. The coordinated SPM method presents an interesting area of research worthy of further attention, and below a few directions of future research have been identified.

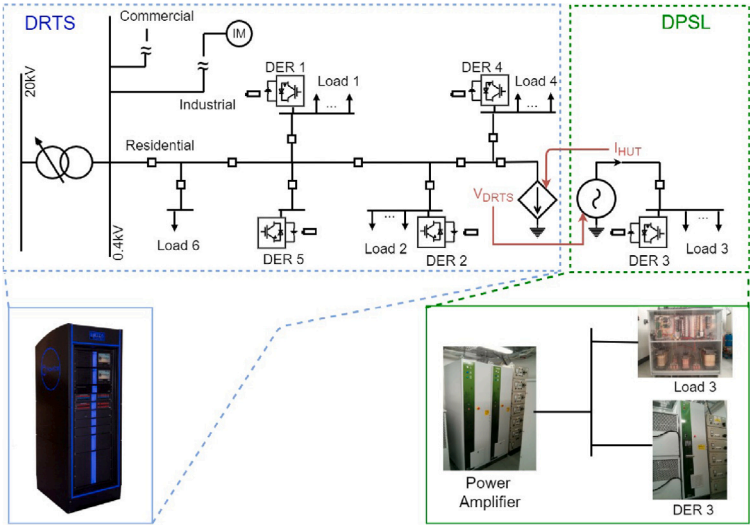

(a) PHIL implementation diagram.

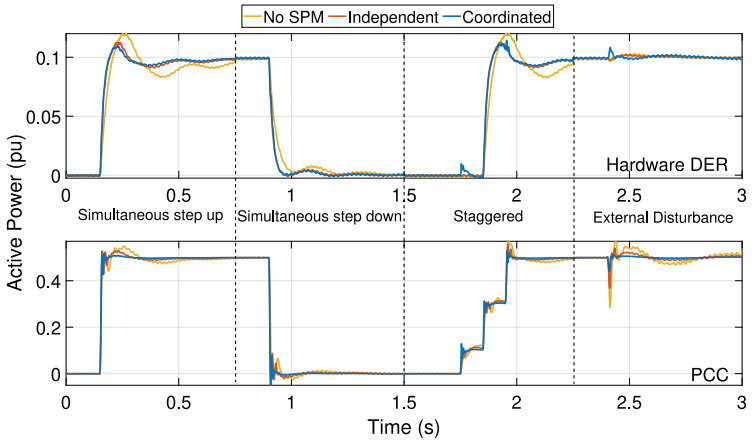

(b) PHIL evaluation results.

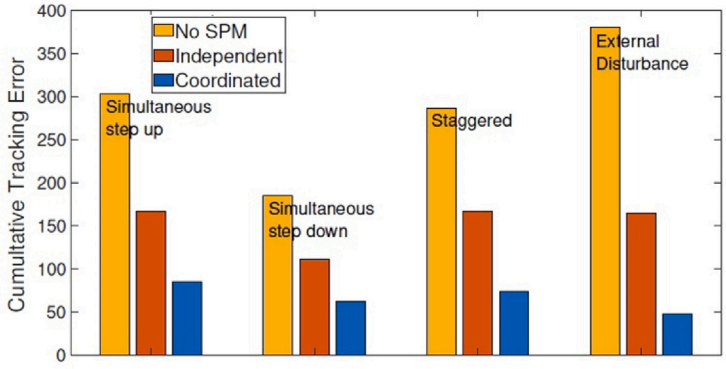

(c) CTE for scenarios under consideration - PHIL.

Fig. 8. PHIL performance evaluation.

- The proposed approach and intended application cater for the desired properties to ensure performance under distributed communications. The reliability and scalability of the approach can be further enhanced by reducing the reliance of the approach upon communications. To this end, three future directions are identified: (i) implementation of the proposed control through a consensus approach aimed at reducing communication burden within the network, (ii) incorporation of methods to optimize the communication network architecture based on the power system requirements; and (iii) implementation of distributed control through the incorporation of DER digital twins.
- The performance of the approach has been verified within an LVAC distribution network and a DC microgrid independently, demonstrating its flexibility for adoption within different networks. The use of the approach for hybrid AC/DC network architectures has not yet been explored. Many articles in literature have proposed coordinated control for hybrid AC/DC microgrids

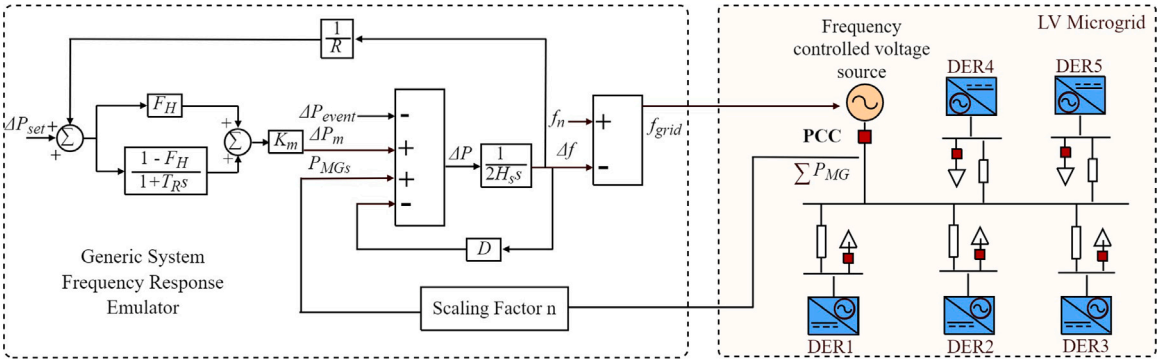

Fig. 9. Illustration of frequency regulation study incorporating generic frequency response emulator.

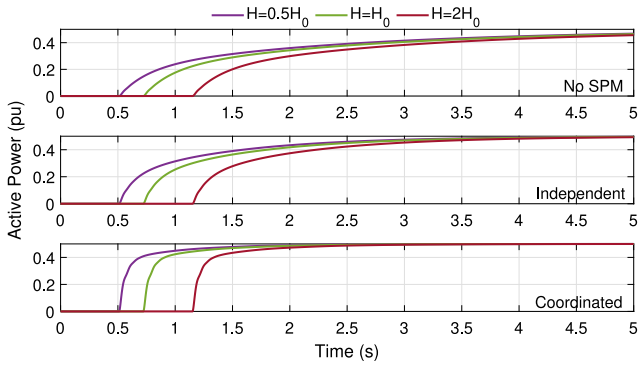

(a) Sum of active power responses of DER.

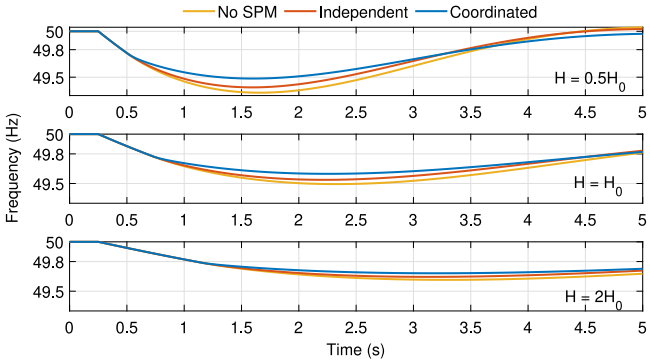

(b) Frequency response of the transmission network.

Fig. 10. Evaluation of proposed approach for grid frequency regulation.

where the focus has been on coordinating the power flow between the two subgrids [50,51], but very limited literature is available on hybrid AC/DC microgrid participation in provision of ancillary services [52]. The proposed approach holds potential for improving the combined response of such networks, particularly by means of harnessing the fast response speed of DC converters (subject to capacities and the response speed of the interfacing converter). Furthermore, the incorporation of the independent SPM can improve the dynamics of power management controls between the AC and DC subgrids. These, in addition to comprehensive stability analysis, remain interesting topics to be further explored.

- Most modern power electronic converters interfacing DER have the ability to be overloaded up to 150% of their rated power capacity for a short period of time. This capability can be harnessed to support devices with slower dynamic response. However, the financial modelling of incentivizing the short-term additional support remains to be explored and implications analysed.

7. Conclusions

In this paper, a two-level coordinated set point modulation (SPM) approach to enhance the cumulative dynamic response of distributed DERs participating in ancillary service provision at a chosen point of common coupling (PCC) is proposed. The performance of the proposed approach is benchmarked against conventional approach where no SPM is incorporated. It has been shown that both levels of control, independent and coordinated, perform significantly better than the conventional approach. Level I control improves the local response of the participating DER, however does not help the cumulative response at the PCC. The coordinated approach in contrast improves the local dynamic response and the cumulative dynamic response at the PCC. The performance of the approach has been verified within a LVAC

Table A.5
Generic system frequency response emulator parameters.

Variables	Description	
ΔP_{set}	Synchronous generator change in power set point	
ΔP_m	Change in mechanical power output	
Δf	Change in grid frequency	
f_{grid}	Grid frequency	
Constants	**Description**	**Value**
F_H	Fraction of power generated by the turbine	0.1
T_R	Turbine reheat time constant	4 s
K_m	Mechanical power gain factor	0.95
ΔP_{event}	Change of power due to events	100 MW
H_s	Inertia constant	2 s
R	Droop constant	0.05
D	Damping constant	0.06
f_n	Nominal frequency	50 Hz

$H_s = H_0$ for the case study in Section V.

distribution network and a DC distribution network, demonstrating its flexibility for adoption within different networks. The real-world applicability of the approach has further been demonstrated through a high fidelity power hardware-in-the-loop experimental validation. In addition, the potential role of the proposed approach in frequency regulation of a transmission network has been demonstrated. The proposed control will allow virtual power plants to ensure tighter set point tracking at PCC's of interest such as the distribution-transmission interface and to participate in markets with more stringent time and regulation requirements as expected in future low-inertia systems.

CRediT authorship contribution statement

Mazheruddin Syed: Conceptualization, Methodology, Investigation, Validation, Formal analysis, Writing – original draft, Funding acquisition. **Ali Mehrizi-Sani:** Conceptualization, Methodology, Writing – original draft, Funding acquisition. **Maria Robowska:** Visualization, Investigation. **Efren Guillo-Sansano:** Writing – review & editing. **Dong Wang:** Investigation, Validation, Writing – original draft. **Graeme Burt:** Supervising, Funding acquisition.

Declaration of competing interest

The authors declare that they have no known competing financial interests or personal relationships that could have appeared to influence the work reported in this paper.

Acknowledgements

This work was supported in part by the European Commission under the H2020 Programme's ERIGRID and ERIGRID2.0 projects (grant no: 654113 and 870620), in part by National Science Foundation (NSF) award ECCS-1953198, in part by the U.S. Department of Energy's (DOE) Office of Energy Efficiency and Renewable Energy (EERE) under the Solar Energy Technologies Office award number 38637 , and in part by the Commonwealth Cyber Initiative (CCI), Commonwealth of Virginia.

Appendix

The definitions of the parameters of the generic system frequency response emulator are presented in Table A.5, along with the values of constants utilized for the case study in Section 5.

The LV microgrid adopted for grid frequency regulation study in Section 5 is an adaptation of the LVAC feeder presented in Fig. 2. The commercial and the industrial feeder branches have been omitted, and only buses with DERs have been considered. The response characteristics of DERs have been adjusted to reflect two fast acting DERs (rise time <0.5 s) within the microgrid with other three presenting slower dynamic response (rise time >4 s).

References

[1] Ofgem. Technical Report on the events of 9 August 2019, [Online]. Available: https://www.ofgem.gov.uk/system/files/docs/2019/09/eso_technical_report_-_final.pdf.
[2] National electricity transmission system security and quality of supply standard. 2021, [Online]. Available: https://www.nationalgrideso.com/industry-information/codes/security-and-quality-supply-standards/code-documents.
[3] Lundstrom B, Patel S, Attree S, Salapaka MV. Fast primary frequency response using coordinated DER and flexible loads: Framework and residential-scale demonstration. In: 2018 IEEE power energy society general meeting. 2018, p. 1–5.
[4] IET. Electricity networks - Handling a shock to the system. [Online]. Available: https://www.theiet.org/media/2785/elec-shock-tech.pdf.
[5] Khan MAU, Hong Q, Liu D, Egea-Àlvarez A, Avras A, Dyśko A, et al. Experimental assessment and validation of inertial behaviour of virtual synchronous machines. IET Renew Power Gener 2022. [Online]. Available: https://ietresearch.onlinelibrary.wiley.com/doi/abs/10.1049/rpg2.12496.
[6] Hosseinzadeh N, Aziz A, Mahmud A, Gargoom A, Rabbani M. Voltage stability of power systems with renewable-energy inverter-based generators: A review. Electronics (Switzerland) 2021;10(2):1–27.
[7] Pepermans G, Driesen J, Haeseldonckx D, Belmans R, D'haeseleer W. Distributed generation: Definition, benefits and issues. Energy Policy 2005;33(6):787–98, [Online]. Available: https://www.sciencedirect.com/science/article/pii/S0301421503003069.
[8] Dondi P, Bayoumi D, Haederli C, Julian D, Suter M. Network integration of distributed power generation. J Power Sources 2002;106(1):1–9, [Online]. Available: https://www.sciencedirect.com/science/article/pii/S037877530101031X, Proceedings of the Seventh Grove Fuel Cell Symposium.
[9] Dugan R, McDermott T, Ball G. Distribution planning for distributed generation. In: 2000 Rural electric power conference. Ppapers presented at the 44th annual conference (Cat. No.00CH37071). 2000, p. C4/1–7.
[10] Mir AS, Senroy N. Intelligently controlled flywheel storage for enhanced dynamic performance. IEEE Trans Sustain Energy 2019;10(4):2163–73.
[11] Short JA, Infield DG, Freris LL. Stabilization of grid frequency through dynamic demand control. IEEE Trans Power Syst 2007;22(3):1284–93.
[12] Karbouj H, Rather Z, Flynn D, Qazi H. Non-synchronous fast frequency reserves in renewable energy integrated power systems: A critical review. Int J Electr Power Energy Syst 2019;106:488–501.
[13] Meyn SP, et al. Ancillary service to the grid using intelligent deferrable loads. IEEE Trans Automat Control 2015;60(11):2847–62.
[14] Ortega-Vazquez MA, et al. Electric vehicle aggregator/system operator coordination for charging scheduling and services procurement. IEEE TransPower Syst 2013;1806–15.
[15] Hao H, et al. Aggregate flexibility of thermostatically controlled loads. IEEE Trans Power Syst 2015;30(1):189–98.
[16] Galus MD, et al. Provision of load frequency control by PHEVs, controllable loads, and a cogeneration unit. IEEE Trans Ind Electron 2011;58(10):4568–82.
[17] Mashhour E, et al. Bidding strategy of virtual power plant for participating in energy and spinning reserve markets—Part I: Problem formulation. IEEE Trans Power Syst 2011;949–56.
[18] Mashhour E, et al. Bidding strategy of virtual power plant for participating in energy and spinning reserve markets—Part II: Numerical analysis. IEEE Trans Power Syst 2011;26(2):957–64.
[19] Moutis P, et al. Decision trees-aided active power reduction of a virtual power plant for power system over-frequency mitigation. IEEE Trans Ind Inf 2015;11(1):251–61.
[20] Etherden N, et al. Virtual power plant for grid services using IEC 61850. IEEE Trans Ind Inf 2016;437–47.
[21] Li P, et al. A robust distributed economic dispatch strategy of virtual power plant under cyber-attacks. IEEE Trans Ind Inf 2018;14(10):4343–52.
[22] Dall'Anese E, et al. Photovoltaic inverter controllers seeking AC optimal power flow solutions. IEEE Trans Power Syst 2016;31(4):2809–23.
[23] Bernstein A, et al. A composable method for real-time control of active distribution networks with explicit power setpoints. Part I: Framework. Electr Power Syst Res 2015;125:254–64.
[24] Dall'Anese E, et al. Optimal regulation of virtual power plants. IEEE Trans Power Syst 2018;33(2):1868–81.
[25] Aien M, et al. On possibilistic and probabilistic uncertainty assessment of power flow problem: A review and a new approach. Renew Sustain Energy Rev 2014;37:883–95.
[26] Khalesi N, et al. Dg allocation with application of dynamic programming for loss reduction and reliability improvement. Int J Electr Power Energy Syst 2011;288–95.
[27] Abdelaziz AY, et al. Optimal planning of distributed generators in distribution networks using modified firefly method. Electr Power Compon Syst 2015;43(3):320–33.
[28] Trovão JPF, et al. A real-time energy management architecture for multisource electric vehicles. IEEE Trans Ind Electron 2015;62(5):3223–33.

[29] Song M, et al. Multi-time-scale modeling and parameter estimation of TCLs for smoothing out wind power generation variability. IEEE Trans Sustain Energy 2019;10(1):105–18.
[30] Syed MH, Guillo-Sansano E, Mehrizi-Sani A, Burt GM. Facilitating the transition to an inverter dominated power system: Experimental evaluation of a non-intrusive add-on predictive controller. Energies 2020;13(16). [Online]. Available: https://www.mdpi.com/1996-1073/13/16/4237.
[31] Yazdanian M, Mehrizi-Sani A, Seebacher RR, Krischan K, Muetze A. Smooth reference modulation to improve dynamic response in electric drive systems. IEEE Trans Power Electron 2018;33(7):6434–43.
[32] Ghaffarzadeh H, Stone C, Mehrizi-Sani A. Predictive set point modulation to mitigate transients in lightly damped balanced and unbalanced systems. IEEE Trans Power Syst 2017;32(2):1041–9.
[33] Mehrizi-Sani A, et al. Online set point modulation to enhance microgrid dynamic response: Theoretical foundation. IEEE Trans Power Syst 2012;27(4):2167–74.
[34] Ghaffarzadeh H, et al. Predictive set point modulation to mitigate transients in lightly damped balanced and unbalanced systems. IEEE Trans Power Syst 2017;32(2):1041–9.
[35] Yazdanian M, et al. Smooth reference modulation to improve dynamic response in drive systems. IEEE Trans Power Electron 2018;6434–43.
[36] Lian F-L, Moyne J, Tilbury D. Network design consideration for distributed control systems. IEEE Trans Control Syst Technol 2002;10(2):297–307.
[37] Park P, Coleri Ergen S, Fischione C, Lu C, Johansson KH. Wireless network design for control systems: A survey. IEEE Commun Surv Tutor 2018;20(2):978–1013.
[38] Zhou Q, Shahidehpour M, Paaso A, Bahramirad S, Alabdulwahab A, Abusorrah A. Distributed control and communication strategies in networked microgrids. IEEE Commun Surv Tutor 2020;22(4):2586–633.
[39] Global ping statistics. 2020, https://wondernetwork.com/pings. [Accessed 09 April 2020].
[40] Mehrizi-Sani A, et al. Performance evaluation of a distributed control scheme for overvoltage mitigation. In: CIGRÉ int. symp. electric power syst. of future: Integrating supergrids and microgrid. Bologna, Italy; 2011.
[41] Unruh P, Nuschke M, Strauß P, Welck F. Overview on grid-forming inverter control methods. Energies 2020;13(10). [Online]. Available: https://www.mdpi.com/1996-1073/13/10/2589.
[42] Olivares D, Mehrizi-Sani A, Etemadi A, Canizares C, Iravani R, Kazerani M, et al. Trends in microgrid control. IEEE Trans Smart Grid 2014;5(4):1905–19.
[43] Strunz K, et al. Benchmark systems for network integration of renewable energy resources. CIGRÉ Task Force C 2014;6(04–02):119.
[44] Papathanassiou S, Hatziargyriou N, Strunz K. A benchmark low voltage microgrid network. In: CIGRÉ symposium 2005. Athens, Greece; 2010.
[45] Emhemed AAS, Burt GM. An advanced protection scheme for enabling an LVDC last mile distribution network. IEEE Trans Smart Grid 2014;5(5):2602–9.
[46] Wang D, Psaras V, Emhemed AAS, Burt GM. A novel fault let-through energy based fault location for LVDC distribution networks. IEEE Trans Power Deliv 2021;36(2):966–74.
[47] Wang D, Emhemed AAS, Burt GM. Improved voltage-based protection scheme for an LVDC distribution network interfaced by a solid state transformer. IET Gener, Transm Distrib 2019;13(21):4809–20.
[48] Kotsampopoulos P, et al. A benchmark system for hardware-in-the-loop testing of distributed energy resources. IEEE Power Energy Technol Syst J 2018;5(3):94–103.
[49] Hong Q, Nedd M, Norris S, Abdulhadi I, Karimi M, Terzija V, et al. Fast frequency response for effective frequency control in power systems with low inertia. J Eng 2019;2019:1696–702.
[50] Nejabatkhah F, Li YW. Overview of power management strategies of hybrid AC/DC microgrid. IEEE Trans Power Electron 2015;30(12):7072–89.
[51] Gupta A, Doolla S, Chatterjee K. Hybrid AC–DC microgrid: Systematic evaluation of control strategies. IEEE Trans Smart Grid 2018;9(4):3830–43.
[52] Maza-Ortega JM, Mauricio JM, Barragán-Villarejo M, Demoulias C, Gómez-Expósito A. Ancillary services in hybrid AC/DC low voltage distribution networks. Energies 2019;12(19). [Online]. Available: https://www.mdpi.com/1996-1073/12/19/3591.